HHS Public Access

Author manuscript

Nature. Author manuscript; available in PMC 2018 March 28.

Published in final edited form as:

Nature. 2017 September 28; 549(7673): 528–532. doi:10.1038/nature23910.

Maternal gut bacteria promote neurodevelopmental abnormalities in mouse offspring

Sangdoo Kim[1,*], **Hyunju Kim**[1,*], **Yeong S. Yim**[2], **Soyoung Ha**[1], **Koji Atarashi**[3], **Tze Guan Tan**[4], **Randy S. Longman**[5], **Kenya Honda**[3], **Dan R. Littman**[6,7], **Gloria B. Choi**[2], and **Jun R. Huh**[1,†]

[1]Division of Infectious Diseases and Immunology and Program in Innate Immunity, Department of Medicine, University of Massachusetts Medical School, Worcester, MA 01605, USA

[2]The McGovern Institute for Brain Research, Department of Brain and Cognitive Neurosciences, Massachusetts Institute of Technology, Cambridge, MA 02139, USA

[3]Department of Microbiology and Immunology, Keio University School of Medicine, Tokyo 160-8582, Japan

[4]Department of Microbiology and Immunobiology, Harvard Medical School, Boston, MA 02115, USA

[5]Jill Roberts Center for IBD, Weill Cornell Medicine, New York, NY 10021, USA

[6]The Kimmel Center for Biology and Medicine of the Skirball Institute, New York University School of Medicine, New York, NY 10016, USA

[7]Howard Hughes Medical Institute, New York, NY 10016, USA

Abstract

Maternal immune activation (MIA) contributes to behavioral abnormalities associated with neurodevelopmental disorders in both primate and rodent offspring[1-4]. In humans, epidemiological studies suggest that exposure of fetuses to maternal inflammation increases the likelihood of developing Autism Spectrum Disorder (ASD)[5-7]. We recently demonstrated that interleukin-17a (IL-17a) produced by Th17 cells, $CD4^+$ T helper effector cells involved in multiple inflammatory conditions, is required in pregnant mice to induce behavioral as well as cortical abnormalities in the offspring exposed to MIA[8]. However, it is unclear if other maternal factors are required to

Correspondence and requests for materials should be addressed to G.B.C. (gbchoi@mit.edu) and J.R.H. (jun.huh@umassmed.edu).
†Present address: Division of Immunology, Department of Microbiology and Immunobiology, Harvard Medical School, Boston, MA 02115, USA and Evergrande Center for Immunological Diseases, Harvard Medical School and Brigham and Women's Hospital, Boston, MA 02115, USA
*These authors contributed equally to this work.

Supplementary Information is attached.

Author Contributions S.K., T.G.T, K.H., D.R.L., G.B.C. and J.R.H. designed the experiments and/or provided advice, reagents and technical expertise. S.K., H.K., Y.S.Y., S.H. and K.A. performed the experiments. S.K., G.B.C. and J.R.H. wrote the manuscript with inputs from the co-authors.

The authors declare no competing financial interests. Readers are welcome to comment on the online version of the paper.

promote MIA-associated phenotypes. Moreover, underlying mechanisms by which MIA leads to T cell activation with increased IL-17a in the maternal circulation are not well understood. Here, we show that MIA phenotypes in offspring require maternal intestinal bacteria that promote Th17 cell differentiation. Pregnant mice that had been colonized with the mouse commensal segmented filamentous bacteria (SFB) or human commensal bacteria that induce intestinal Th17 cells were more likely to produce offspring with MIA-associated abnormalities. We also show that small intestine dendritic cells (DCs) from pregnant, but not from non-pregnant, females upon exposure to MIA secrete IL-1β/IL-23/IL-6 and stimulate T cells to produce IL-17a. Overall, our data suggest that defined gut commensal bacteria with a propensity to induce Th17 cells may increase the risk for neurodevelopmental disorders in offspring of pregnant mothers undergoing immune system activation due to infections or autoinflammatory syndromes.

In mouse models of MIA, offspring born to pregnant dams exposed to viral infection or injected with a synthetic double-stranded RNA (polyinosinic:polycytidylic acid, poly(I:C)), which mimics viral infection, exhibit abnormal behavioral phenotypes, including reduced sociability, increased repetitive behaviors, and abnormal communication[3,4]. Because commensal microbiota influences immune responses to pathogenic microbes, we wished to determine if it affects the mother's likelihood of producing offspring with MIA-associated phenotypes.

As previously reported[8-10], pups from mothers injected with poly(I:C) at embryonic day 12.5 (E12.5) emit more ultrasonic vocalization (USV) calls than those from PBS-injected mothers (Fig. 1a). Unlike other behavioral phenotypes that are often more strongly manifested in male than in female offspring, USV calls were enhanced in both sexes among MIA offspring (Extended Data Fig. 1a). In addition, fetal exposure to MIA led to other behavioral abnormalities including enhanced repetitive behaviors (increased marble burying), increased anxiety (decreased time spent in the center of an open field arena) and social interaction deficits (decreased interaction with a social stimulus) in adult male offspring (Fig. 1b-d). These behavioral phenotypes did not emerge from changes in activity or arousal levels as the total investigation time and the total distance traveled during the sociability test remained comparable (Extended Data Fig. 1b and c). To investigate whether maternal commensal bacteria influence MIA-associated behaviors, we treated C57BL/6 wildtype (WT) mice from our vivarium with the broad spectrum antibiotic vancomycin prior to phosphate-buffered saline (PBS) or poly(I:C) administration (Extended Data Fig. 1d). Interestingly, pre-treating poly(I:C)-injected mothers with vancomycin prevented development of all four behavioral abnormalities in MIA offspring (Fig. 1a-d).

We previously showed that MIA offspring exhibit cortical patches devoid of cortical layer-specific markers, such as SATB2[8], and these cortical patches resemble lesions described in brains of ASD patients[11,12]. These cortical patches are predominantly localized in the area encompassing the dysgranular zone of the primary somatosensory cortex (S1DZ) and are closely associated with the MIA-associated behavioral abnormalities (Yim et al., co-submitted manuscript). Unlike the adult offspring derived from poly(I:C)-injected dams, the offspring of poly(I:C)-injected mothers pre-treated with vancomycin failed to develop cortical patches (Fig. 1e and Extended Data Fig. 1e, f). Vancomycin treatment of poly(I:C)-

injected pregnant dams led to a decrease in the proportion of Th17 cells in the small intestine with a concomitant reduction in the levels of IL-17a in the maternal plasma, compared to those of the control group (Fig. 1f and Extended Data Fig. 1g). These data indicate that the presence in pregnant mice of commensal bacteria sensitive to vancomycin is crucial for the induction of MIA-associated behavioral and brain abnormalities in the offspring. Furthermore, the presence of such bacteria is associated with increased proportion of Th17 cells in the small intestines and high levels of IL-17a in the plasma of poly(I:C)-treated pregnant dams.

Among commensal bacteria in laboratory mice, SFB is susceptible to vancomycin[13] and contributes disproportionately to Th17 cell biogenesis in the small intestine[14]. Indeed, qPCR analyses of mouse fecal samples showed that intestinal colonization by SFB is severely reduced upon vancomycin treatment (Extended Data Fig. 1h). We also performed scanning electron microscopy (SEM) to visualize SFB, which is associated with intestinal epithelial cells (IEC)[14]. Whereas plenty of SFB were found attached to the ileal mucosa of the PBS-treated dams, IEC-associated SFB were not detected in the vancomycin-treated dams (Extended Data Fig. 1i). We therefore next investigated if the presence of SFB in pregnant mice correlated with the MIA-associated behavioral phenotypes in offspring. C57BL/6 mice from Taconic Biosciences (Tac) have abundant Th17 cells in their small intestine due to the presence of SFB; in contrast, C57BL/6 mice from Jackson Laboratories (Jax), which lack SFB, have few intestinal Th17 cells[13,14]. Unlike offspring from poly(I:C)-injected Tac mothers, those from poly(I:C)-injected Jax mothers failed to show any of the MIA-associated behavioral phenotypes (Fig. 2a-d and Extended Data Fig. 2a, b). Poly(I:C)-treated Tac versus Jax mothers had litters of similar size and the pups had similar weights (Extended Data Fig. 2c, d). Sizes of the cortical patches observed in the offspring of poly(I:C)-injected Tac mothers were highly correlated with the severity of the MIA-associated behavioral abnormalities (Yim et al., co-submitted manuscript). Consistent with this finding, MIA offspring from the SFB-deficient Jax mothers injected with poly(I:C) had no cortical abnormalities, as assessed by SATB2 staining (Fig. 2e and Extended Data Fig. 2e, f). Unlike in Tac mice, Jax mothers injected with poly(I:C) did not show systemic increases in IL-17a in the plasma (Fig. 2f). However, poly(I:C) injection of both Tac and Jax animals resulted in the robust induction of TNF-α and IFN-β, compared to PBS control mice (Extended Data Fig. 2g).

Offspring of poly(I:C)-injected Jax mothers that had been either co-housed with Tac mice or gavaged with a fecal slurry from SFB mono-colonized mice (Extended Data Fig. 3a) displayed MIA-associated behavioral and cortical abnormalities (Fig. 2a-e). These MIA-associated phenotypes in the offspring from both the co-housed as well as SFB-gavaged Jax mothers were accompanied by increased proportion of gut-residing Th17 cells, consistent with the presence of SFB in the small intestine of these mice (Extended Data Fig. 3b-d). Accordingly, the co-housed and SFB-gavaged Jax mothers exhibited increased levels of plasma IL-17a following poly(I:C) injections (Fig. 2f). Thus, the presence or absence of a single commensal bacterial species SFB in the intestines of pregnant mothers influences long-lasting behavioral and neurodevelopmental outcomes in the offspring exposed to MIA.

We next investigated if maternal exposure to poly(I:C)-induced inflammation or maternal colonization with SFB influence MIA-associated behaviors in offspring after birth. We performed cross-fostering experiments by switching newborns between PBS- and poly(I:C)-treated Tac mothers or between SFB-positive Tac and SFB-negative Jax mothers (Extended Data Fig. 4a and 5a). Whereas offspring derived from poly(I:C)-injected mothers, but reared by PBS-injected mothers, exhibited behavioral abnormalities, those from PBS-injected mothers that were reared by poly(I:C) mothers exhibited normal behaviors (Extended Data Fig. 4b-g). Likewise, offspring derived from poly(I:C)-injected Tac mothers, but reared by Jax mice, exhibited behavioral abnormalities, whereas those derived from poly(I:C)-injected Jax mothers and reared by Tac mothers displayed normal behaviors (Extended Data Fig. 5b-g). These data indicate that the presence of SFB in the small intestine of mothers as well as the immunological effects of poly(I:C) are critical during pregnancy, not during post-natal nursing, for licensing MIA-induced behavioral abnormalities in offspring.

MIA leads to an increase in plasma IL-17a levels in pregnant mice as early as 12-24 h following E12.5 poly(I:C) injection[8]. Such a rapid increase strongly suggested that pre-existing Th17 cells, rather than *de novo* differentiating Th17 cells, are the major source for IL-17a in pregnant mice exposed to inflammation. As Th17 cells are most abundant in the small intestine lamina propria, we next investigated whether poly(I:C) stimulates IL-17a production via gut-residing Th17 cells. In poly(I:C)-treated pregnant mice, T cells isolated from lamina propria, but not spleen or mesenteric lymph node, expressed high levels of IL-17a and had increased RORγt expression as compared to cells from PBS-treated mice (Extended Fig. 6a-f). Consistent with these observations, ileum-associated mononuclear cells, isolated from poly(I:C)-injected Tac pregnant mice and further stimulated *in vitro* with poly(I:C), produced higher levels of IL-17a compared to those from PBS-treated Tac mice (Extended Data Fig. 6g and Fig. 3a). In contrast, mononuclear cells from poly(I:C)-treated Jax mice secreted only small amounts of IL-17a (Fig. 3a). Introduction of SFB into Jax mice either by co-housing them with Tac mice or by gavaging them with an SFB-containing fecal slurry was sufficient to enable ileum-associated mononuclear cells to produce high levels of IL-17a (Fig. 3a). To examine which cells are involved in the poly(I:C) response, we separately isolated $CD4^+$ as well as non-$CD4^+$ cells from PBS- and poly(I:C)-treated pregnant Tac mice and co-cultured the isolated cells from each experimental group. The non-$CD4^+$ fraction derived from the poly(I:C)-, but not from the PBS-treated mothers, promoted IL-17a production when added to cultures containing $CD4^+$ cells from either PBS- or poly(I:C)- treated pregnant mice (Extended Data Fig. 6h). We next tested if poly(I:C)-primed $CD11c^+$ DC cells were capable of supporting $CD4^+$ T cells to produce IL-17a. Adding $CD11c^+$ cells derived from poly(I:C)-, but not from PBS-treated, pregnant mice to *ex vivo* cultures containing ileal $CD4^+$ T cells that were isolated from either PBS- or poly(I:C)-treated pregnant Tac mice led to robust expression of IL-17a (Fig. 3b). In contrast, neither splenic $CD4^+$ T cells of poly(I:C)-injected pregnant Tac mice nor ileal $CD4^+$ T cells of poly(I:C)-injected pregnant Jax mice produced IL-17a even with the help of $CD11c^+$ cells (Fig. 3b). Thus, both $CD4^+$ T cells present in the small intestines of Tac mice and poly(I:C)-activated $CD11c^+$ cells are required for robust IL-17a induction. Among the multiple phenotypes of gut-residing DCs, $CD103^+CD11b^+CD11c^+$ cells were robust inducers of

IL-17a when co-cultured with ileal $CD4^+$ T cells (Extended Data Fig. 6i), consistent with previous reports[15,16].

Because poly(I:C) activates Toll-like receptor 3 (TLR3)[17], we investigated if this receptor is involved in stimulation of IL-17a production. Whereas $CD4^+$ T cells, regardless of their *tlr3* genotype, produced IL-17a when mixed with WT $CD11c^+$ cells, they failed to do so when co-cultured with TLR3-deficient $CD11c^+$ DCs (Fig. 3c). In addition, poly(I:C) injection to TLR3 KO pregnant mice failed to induce MIA-associated USV phenotypes in offspring (Extended Data Fig. 6j). These data suggest that MIA-associated phenotypes require functional TLR3 expression on gut $CD11c^+$ DC.

Inflammatory cytokines such as IL-1β/IL-6/IL-23 enhance Th17 cell function and differentiation[18]. Consistent with this notion, co-cultures of sorted $CD4^+$ and $CD11c^+$ DCs that were isolated from the ilea of poly(I:C)-treated gravid Tac mice and incubated with IL-1β/IL-6/IL-23 blocking antibodies failed to produce IL-17a, even when supplemented with poly(I:C) (Fig. 3d). In contrast, GFP^+ Th17 cells, but not GFP^- non-Th17 cells, sorted from the ilea of IL-17a-GFP reporter mice, produced high levels of IL-17a in the presence of exogenous IL-1β/IL-6/IL-23, even in the absence of poly(I:C)-treated $CD11c^+$ cells (Fig. 3e). Collectively, these data indicate that poly(I:C) treatment leads to the activation of gut-residing $CD103^+CD11b^+CD11c^+$ cells, which stimulate poised Th17 cells to produce IL-17a through secretion of IL-1β/IL-6/IL-23.

Intriguingly, we noted that poly(I:C) injection of non-pregnant females failed to increase the levels of plasma IL-17a (Fig. 3f). Co-culture of ileal $CD4^+$ and $CD11c^+$ cells isolated from poly(I:C)-treated pregnant females, but not from poly(I:C)-treated non-pregnant females, resulted in secretion of IL-17a *ex vivo* (Fig 3g). Consistent with these findings, gut $CD11c^+$ DCs isolated from poly(I:C)-treated pregnant females, but not from poly(I:C)-treated non-pregnant females, produced increased levels of IL-1β/IL-6/IL-23 (Extended Data Fig. 6k). In sum, these data collectively suggest that Th17 cell-inducing gut bacteria, a pro-inflammatory stimulus and pregnancy are all required for the systemic increase of IL-17a in maternal plasma, which promotes MIA-associated behavioral and neurodevelopmental abnormalities in offspring.

We next investigated whether commensal-antigen specific Th17 cells in pregnant mothers are sufficient to induce MIA-associated phenotypes in the offspring. Congenically marked naïve $CD45.1^+CD4^+$ T cells from mice expressing a transgenic T cell receptor (TCR) specific for a SFB-encoded antigen (7B8 Tg)[19] were adoptively transferred into SFB-colonized $CD45.2^+$ recipient mice lacking αβ T cells (TCRα KO) or deficient for IL-17a production (IL-17a KO) (Extended Data Fig. 7a). In line with our previous findings that Th17 cells are critical mediators of MIA[8], offspring derived from poly(I:C)-injected TCRα KO mothers crossed with B6 WT fathers failed to exhibit MIA-induced behavioral phenotypes. On the other hand, offspring from TCRα KO pregnant mothers that had received naïve 7B8 $CD4^+$ T cells exhibited MIA-associated behavioral phenotypes even in the absence of exposure to poly(I:C)-induced inflammation (Extended Data Fig. 7b). We subsequently tested if IL-17a produced by the SFB antigen-specific $CD4^+$ T cells was sufficient to induce MIA phenotypes in offspring by transferring these cells into IL-17a KO

females[20]. Unlike the offspring from the poly(I:C)-treated IL-17a KO mothers that had been crossed with B6 WT fathers, offspring of poly(I:C)-injected IL-17a KO mothers that had received 7B8 $CD4^+$ T cells displayed all four MIA-associated behavioral abnormalities (Extended Data Fig. 7c). In addition, offspring from 7B8 $CD4^+$ T cell recipient females exhibited the cortical phenotype (Extended Data Fig. 7d-h). Induction of the MIA behavioral phenotypes was accompanied by an increase in IL-17a in the maternal plasma (Extended Data Fig. 7i, j) and increased IL-17a production from SFB-specific donor $CD45.1^+$ T cells, but not from $CD45.2^+$ T cells of IL-17a KO recipient mice (Extended Data Fig. 7k). Therefore, these results indicate that microbiota-specific gut Th17 cells present in pregnant mice are sufficient to produce abnormal behavioral and neurodevelopmental phenotypes in the offspring when accompanied by strong signaling for IL-17a production in the mother.

Lastly, we investigated if gut-residing bacteria isolated from humans could also promote MIA-associated phenotypes in mice. Administration of a mix of twenty different commensal bacteria isolated from human fecal samples was previously shown to induce Th17 cells in the large intestines of mice[21]. We orally gavaged Jax mothers with a mix of these twenty human bacterial strains twice, on E3.5 and E10.5, followed by a poly(I:C) injection at E12.5 (Extended Data Fig. 8a). Introduction of the twenty strains led to stable colonization of 2-10 commensal bacteria (Supplementaty Table 1) and, as previously shown[21], to an increased percentage of Th17 cells in the colons of the recipient mice (Extended Data Fig. 8b). Unlike in the SFB-colonized Jax mice, we could not detect SFB in the ilea of the recipient mice (Extended Data Fig. 8c). Importantly, poly(I:C) injection of the human bacteria-gavaged Jax mice induced high levels of IL-17a in the maternal plasma and MIA-associated abnormal behavioral and nerurodevelopmental phenotypes in the offspring (Fig. 4 and Extended Data Fig. 8d-g). These MIA-associated phenotypes were not observed if the mothers were pre-treated with IL-17a blocking antibody (Fig. 4 and Extended Data Fig. 8d-g).

There have been several recent reports of individual human commensal bacteria that promote differentiation of intestinal Th17 cells[22,23]. Unlike offspring from Jax mothers colonized with *L. monocytogenes* or *B. fragilis*, in which there is no induction of Th17 cells, offspring of mice colonized with Th17 cell-inducing *B. adolescentis* or an adherent *E. coli* isolate, CD-SpA 2A, emitted enhanced USV calls (Extended Data Fig. 9a-c). The presence of MIA-associated behavioral phenotype in offspring correlated with increased IL-17a in the plasma of poly(I:C)-injected mothers (Extended Data Fig. 9d). On the other hand, pregnant mice gavaged with *L. monocytogenes* had increased IFN-γ production (Extended Data Fig. 9e). None of these human bacteria gavaged mothers were colonized with SFB (Extended Data Fig. 9f). Thus, intestinal Th17 cell induction by individual human commensal bacteria contributes to the development of MIA-associated abnormality in mouse offspring.

Accumulating evidence suggests that the gut commensal microbiota have roles in autoimmune diseases and cancer[24-26]. Moreover, intricate relationships exists between the bacterial community in the gastrointestinal tract and the central nervous system[27-29]. Our findings extend the potential role of the microbiota in influencing the mother's risk of having offspring with neurodevelopmental disorders. Women with gut microbial communities that promote excessive Th17 cell differentiation may therefore be more likely to bear autistic children in the event of pathological inflammation during pregnancy. A better

understanding of the role of the maternal microbiota and pregnancy-associated changes in gut-residing immune cells may provide opportunities to reduce the risk of inflammation-induced neurodevelopmental disorders.

Methods

Animals

All experiments were performed according to Guide for the Care and Use of Laboratory Animals and were approved by the National Institutes of Health and the Committee and Animal Care at University of Massachusetts Medical School. C57BL/6, *tcra* ^{KO}, *tlr3* ^{KO}, *il17a*^{gfp} and SFB-specific TCR Tg (7B8) mice were purchased from Taconic biosciences and Jackson Laboratory. To induce MIA phenotypes, SFB were introduced into mice purchased from Jackson laboratory. *Il17a*^{KO} mice were described elsewhere[20].

Maternal Immune Activation

Mice were mated overnight and females were checked daily for the presence of seminal plugs, noted as embryonic day 0.5. On E12.5, pregnant female mice were weighed and injected with a single dose (20mg/kg; i.p.) of poly(I:C) (Sigma Aldrich) or PBS vehicle. Each dam was returned to its cage and left undisturbed until the birth of its litter. All pups remained with the mother until weaning on postnatal day 21-28 (P21-P28), at which time mice were group housed at a maximum of 5 per cage with same-sex littermates.

Co-housing, SFB-gavaged and antibiotics-gavaged mice

For co-housing experiments, age-matched SFB-absent mice (from Jackson Laboratory) were co-housed with SFB-present mice (from Taconic Biosciences) in sterilized cages for two weeks at a ratio of 2:3, with unrestricted access to food and water. For SFB-gavaging experiments, four fecal pellets of SFB mono-colonized mice (provided by Dan Littman) were dissolved in 20 ml sterile PBS and filtered though a 100 μm cell strainer. 200 μl of fecal suspensions were gavaged via oral route to 4 week-old female Jackson mice. Control mice were gavaged with PBS. The SFB colonization was tested on day 7 following co-housing or SFB-gavaging. For ablation of intestinal bacteria, Taconic-derived female mice were orally gavaged with vancomycin hydrochloride (Fisher) (2.5 mg/kg) every two days, starting 7 days prior to breeding. Mouse fecal pellets were collected and stored at −80 °C before and after vancomycin treatments.

Human commensal bacteria-gavaged mice

Twenty human-associated Th17-inducing bacterial strains were isolated from fecal samples of a patient with ulcerative colitis[21]. Fifteen strains (1A9, 1F8, 1D2, 1F7, 1D4, 2D9, 2E3, 2E1, 1D10, 1E3, 2H6, 2G4, 2G11, 1B11 and 1C2) were grown on Reinforced Clostridial Agar (Oxoid), two strains (1C12, 1E11) were on GAM Agar (Nissui), two strains (1D1, 2F7) were on Schaedler Agar (BD), and one strain (2H11) was on Tryptic Soy Agar (BD). Two days after plating, microbes were scraped from agar plates, suspended in 5 ml of 20% glycerol in PBS, and mixed with equal number of live bacteria (approximately final concentrations of 5×10^8 CFU/ml of each strain). The mixture of twenty bacterial strains were stored at −80°C until use. Pregnant Jax mice were inoculated twice by oral gavages at

E3.5 and E10.5, with 200-300 μl of bacterial suspension. For the IL-17 cytokine blockade experiment, monoclonal IL-17a blocking antibody (clone 50104; R&D) or isotype control antibody (IgG2a, clone 54447; R&D) were administered 8 h before maternal immune activation via i.p. route (300 μg/animal). For colonization with *B. Fragilis*, *B. Adolescentis* and adherent *E. coli* CD-SpA 2A, pregnant Jax mice were inoculated three times by oral gavages at E4.5, E6.5 and E8.5 with 200 μl of bacteria suspension. (approximately final concentrations of 1×10^9 CFU/ml of each strain). Bacterial stocks were prepared as previously described[22,23].

Listeria-gavaged mice

Listeria monocytogenes[19] was cultured in BHI broth media (Sigma, Cat no 35286 cfu). Pregnant Jax mice were inoculated three times by oral gavages at E4.5, E6.5 and E8.5 with 200 μl of bacteria suspension (approximately final concentrations of 2×10^9 CFU/ml). Colonization levels were determined by collecting mouse fecal samples at E12.5, re-suspending them with PBS and subsequently plating on BHI agar.

Cross-fostering

The day on which pups were born was considered P0. Pups were cross-fostered sometime between P0 and P1. Whole litters were removed from the original mothers. Pups were gently mixed with the bedding of the new cage. Pups were then introduced to the new cage with a foster mother. Pups from PBS- and poly(I:C)-treated Taconic mothers were cross-fostered to poly(I:C)- and PBS-treated Taconic mothers, respectively. Additionally, pups from Taconic- and Jax-derived mothers were cross-fostered to a Jax- and Taconic- derived dam, respectively.

Behavioral assays

All behavioral testing were carried out according to the previously established behavioral schemes[8] with minor modifications. Blinding was done for all the behavioral experiments except for the experiments with human bacteria.

Ultrasonic vocalizations—On P9, both male and female offspring mice were removed from the nest and habituated to the testing room for 30 min. After the habituation period, mouse pups were placed in a clean 15cm glass Pyrex high wall dish. Ultrasonic vocalizations (USVs) were detected for 3 min using an UltraSoundGateCM16/CMPA microphone (AviSoft) in the sound attenuation chamber under stable temperature and light control, and recorded with SAS Prolab software (AviSoft). USVs were measured between 33-125kHz using Ultravox software (Noldus information Technology, USA). Due to the unreliability of automated USV scoring, all pup USV calls were counted manually and plotted on the y-axis. Since both male and female pups of poly(I:C)-injected mothers emitted comparable levels of USVs (Extended Data Fig. 1a), we did not separately analyze male versus female USV phenotypes. Both sexes were used for the experiments.

Three-Chamber social approach—8–12-week-old male mice were tested for social behavior using the three-chamber social approach paradigm. Experimental mice were habituated for 1 h in separate clean holding cages and then introduced into a three-chamber

arena with only empty object-containment cages (circular metallic cages, Stoelting Neuroscience) for a total 10-min acclimation phase in two 5 min sessions. The following day the mice were placed in the center chamber (without access to the left and right social test areas) and allowed to explore the center area for 5 min. After this exploration period, barriers to adjacent chambers were removed, allowing mice to explore the left and right arenas, which contained a social object (unfamiliar C57BL/6 male mouse) in one chamber and an inanimate object (black rubber stopper) in the other chamber. Experimental mice were given 10 min to explore both chambers and measured for approach behavior as interaction time (i.e. sniffing, approach) with targets in each chamber (within 2 cm). Sessions were video-recorded and object exploration time and total distance moved were analyzed using the Noldus tracking system. % interaction was calculated as the percentage of time spent investigating the social stimulus out of the total exploration time of both objects (Supplementary Table 2) and plotted on the y-axis. Arenas and contents were thoroughly cleaned between testing sessions. Multiple social targets from different home cages were used for testing to prevent potential odorant confounds from target home cages.

Marble burying test—Male mice were placed in a testing arena (arena size: 40× 20 cm^2, bedding depth: 3 cm) containing 20 glass marbles, which were laid out in four rows of five marbles equidistant from one another. At the end of a 15 min exploration period, mice were gently removed from the testing cages and the number of marbles buried was recorded. A marble burying index was scored as 1 for marbles covered >50% by bedding, 0.5 for ~50% covered, or 0 for anything less. Percentage of buried marbles is plotted on the y-axis.

Open field test—Mice underwent a 15-min exploration period in the testing arena (arena size: 50×50 cm^2). Sessions were video-recorded and analyzed for time spent in the center (center size: 25×25 cm^2) using EthoVision Noldus tracking system (Noldus, Netherlands). Time spent in the center of an open field is plotted on the y-axis.

Immunohistochemistry

Adult male mice were perfused and fixed with 4% paraformaldehyde in PBS for overnight at 4 °C. The brains were removed and sectioned at 50 μm thickness with a Leica VT100S vibratome (Leica, USA). Slices were permeabilized with blocking solution containing 0.4% Triton X-100, 2% goat serum, and 1% BSA in PBS for 1 h at room temperature, and then incubated with anti-SATB2 (special AT-rich sequence-binding protein 2) (ab51502, Abcam) antibodies for overnight at 4°C. The following day, slices were incubated with fluorescently conjugated secondary antibodies (Invitrogen, USA) for 1 h at room temperature, and mounted in vectashield mounting medium with DAPI (Vector Laboratories). Images of stained brain slices were acquired using confocal microscope (LSM710. Carl Zeiss) with a 20X objective lens. The cortical malformation images were analyzed using Image J software. The images were cropped to have S1 cortical patches in the center.

Analysis of cortical patches

Cortical patches were identified as cortical regions devoid of SATB2 expression. The size of the cortical patches in the S1 was calculated using Zen software (Carl Zeiss). The cortical

region was divided into 10 equal laminar blocks representing different depths of the cortex. SATB2 positive cells were quantified manually.

Scanning electron microscopy (SEM)

Terminal ileum tissues from mice (12-14 weeks old) were cut open and fixed with 2.5 % glutaraldehyde in 0.1M cacodylate buffer (pH 7.4) for overnight and processed for standard SEM at EM center, University of Massachusetts Medical School. All samples were taken on a Hitachi S-4800 Type II Field Emission Scanning Electron Microscope.

16S rRNA quantitative PCR analysis

Bacterial genomic DNA was isolated from the fecal pellets of mice with phenol-chloroform extraction. qPCR was performed to quantify relative abundance of SFB, human commensal bacteria or total bacteria using group specific 16S rDNA primers (Supplementaty Table 3). Undetected qPCR values from non-colonized samples were replaced with a Ct value of 40 for the purpose of comparision.

Lamina propria mononuclear cell preparation

For mononuclear cell isolations, both mesenteric fat tissues and Peyer's patches were carefully removed from intestinal tissues. Terminal ileal or colonic tissues were incubated in 5 mM EDTA in PBS containing 1 mM DTT at 37°C on a shaker (200 rpm) for 20 min. Tissues were washed one more time. Tissues were then further digested for 30 min at 37 °C in RPMI containing 10% fetal bovine serum, 1.0 mg/ml Collagenase D (Roche) and 100 μg/ml DNase I (Sigma). Digested tissues were then filtered using a 100 μm cell strainer and incubated for additional 10 min at 37°C. Mononuclear cells were isolated from an interphase of percoll gradients (40:80 gradient).

Flow cytometry

Mononuclear cells were incubated with or without 50 ng/ml phorbol myristate acetate (PMA) (Sigma) and 500 ng/ml ionomycin (Sigma) in the presence of GolgiStop (BD) in complete T cell media at 37°C for 5 h. Intracellular cytokine staining was performed according to the manufacturer's protocol. Cells were stained with Pacific Blue-conjugated anti-CD4 (RM-5), PerCP-Cy5.5-conjugated anti-CD8a (53-6.7), APC-Cy7-conjugated anti-TCRβ (H57-597), FITC-conjugated anti-CD62L (MEL-14), APC-conjugated anti-CD44 (IM7), PE-conjugated-CD25 (PC61.5), PerCP-Cy5.5-conjugated-CD19 (eBio1D3), APC-conjugated anti-CD45.1 (A20), FITC-conjugated anti-CD45.2 (104), Pacific Blue-conjugated anti-CD11c (N418), FITC conjugated-anti-CD11b (M1/70), PerCP-Cy5.5-conjugated-anti-CD103 (2E7) (eBioscience), Biotin-conjugated Vβ14 (14-2) (BD phamigen) and PE-Cy7-conjugated-Streptavidin (Thermo Fisher Scientific). Cells were further stained intracellularly with APC-conjugated anti-RORγ (B2D) (eBioscience) and PE-Cy7-conjugated anti-IL-17a (eBio17B7) (eBioscience) using Foxp3 staining/ permeabilization buffer (eBioscience). Flow cytometric analysis was performed on an LSRII (BD Biosciences). All data were re-analyzed using FlowJo (Tree Star).

Adoptive transfer

Spleen and lymph nodes from 7B8 Tg mice were collected and disassociated. Red blood cells were lysed using ACK lysis buffer (Lonza). Naïve $CD4^+$ T cells ($CD62L^{hi}$ $CD44^{lo}$ $TCRv\beta14^+$ $CD4^+$ $CD19^-$) from $CD45.1^+$ 7B8 Tg mice were sorted on a BD FACS Aria II. Sorted 5×10^4 cells were transferred into congenic CD45.2 recipient mice by tail vein injection.

Cell Sorting

Mononuclear cells were isolated at E14.5 from small intestines of poly(I:C)-treated pregnant *Il-17a*^{gfp} or B6 mice. GFP^+ and GFP^- T cells, gated on $CD8^-$ $CD19^-$ $TCR\beta^+CD4^+$, were sorted with a FACSAria (BD biosciences). DCs were stained with antibodies and sorted based on their surface expression of CD103 and CD11b (gated on $CD4^-$ $CD8^-$ $CD19^-$ $MHCII^+$ $CD11c^+$).

Ex vivo mononuclear cell culture

Mononuclear cells isolated from ilea of either PBS- or poly(I:C)-treated mice on E14.5 were cultured *in vitro* with poly(I:C) (2.5 μg/ml). $CD4^+$ or $CD11c^+$ cells were positively selected using microbeads (Miltenyi). For co-culture assay, $CD4^+$ cells ($1.5 – 3.5 \times 10^4$ cells/mL) were cultured with $CD11c^+$ cells ($7.5 – 16 \times 10^4$ cells/ml) at 1:5 ratio in each well. $CD4^+$ and $CD11c^+$ cells were incubated for 24-48 h with IgG antibody (20 ng/ml) or with anti-IL-1β antibody (20 ng/ml), anti-IL-6 antibody (20 ng/ml) and anti-IL-23p19 antibody (20 ng/ml) (R&D System) with or without poly(I:C) stimulation (2.5 μg/ml) (Sigma). $CD4^+$ cells were cultured with recombinant IL-1β (10ng/ml), IL-6 (5ng/ml) and IL-23 (5ng/ml) (R&D System). All cells were cultured in T cell media: RPMI 1640 (Invitrogen) supplemented with 10% (v/v) heat-inactivated FBS (Hyclone) and 50 U penicillin-streptomycin (Invitrogen). Cell culture supernatant was used for ELISA analyses.

ELISA

IL-17a, TNF-α, IFN-β, IL-1β and IL-23 levels were measured according to the manufacturer's protocol (BioLegend). IL-6 and IFN-γ levels were measured according to the manufacturer's protocol (eBioscience).

Statistics

Statistical analyses were performed using GraphPad Prism. ANOVAs were followed by Tukey or Sidak tests. All data are represented as mean +/− SEM. Sample sizes were determined based on similarly conducted studies[8]. When conducting behavioral assays, cages were pseudo-randomly assigned for tests. Detailed statistical analyses for behavioral assays are listed below.

Data availability statement

Source data are available in the Supplementary information. All other data are available from the corresponding author upon reasonable request.

Extended Data

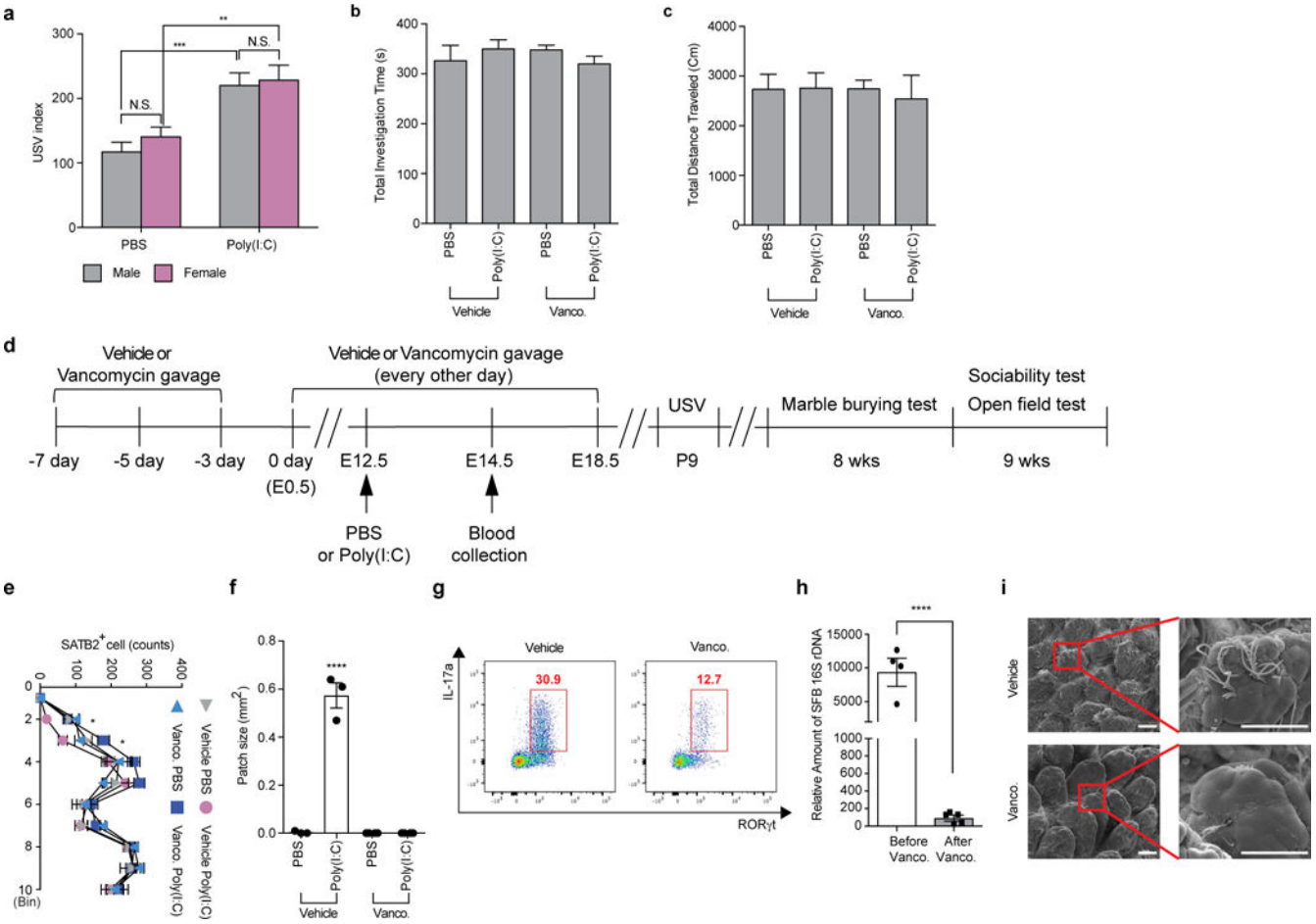

Extended Data Figure 1. Maternal vancomycin-treatment prevented induction of behavioral abnormalities in MIA offspring

a, USV index (n=27/29 (PBS;male/female); n=28/21 (Poly(I:C);male/female); 6 independent experiments). **b-c**, Total investigation time (**b**) and total distance traveled (**c**) during the sociability test (n=13/15 (vehicle;PBS/poly(I:C)); n=12/16 (vancomycin;PBS/poly(I:C)); 3-4 independent experiments). **d**, Schematic of the experimental design. **e-f**, Quantification of SATB2$^+$ cells (**e**) in the cortex divided into ten equal bins representing different depths of the cortex or of the cortical patch size (**f**) in the primary somatosensory cortex (S1) (n=3/4 (PBS;vehicle/vancomycin); n=3/4 (poly(I:C);vehicle/vancomycin); 2 independent experiments). **g**, Flow cytometry of CD4$^+$ T cells (gated on TCR-β$^+$CD4$^+$) stained intracellularly for IL-17a and RORγt. Mononuclear cells were collected at E14.5 from the ilea of poly(I:C)-treated mice with/without vancomycin treatment; Representative FACS plot from 3 independent experiments. **h**, qPCR analysis measuring relative SFB levels in B6 mice before/after vancomycin treatments (n=4-5/group). **i**, Representative SEM images of epithelial surfaces in the ilea of the vehicle-/vancomycin-treated mice from 2 independent experiments. Scale bars, 30 μm. *p<0.05, **p<0.01, ***p<0.001, ****p<0.0001 as calculated by two-way (**a,e**) and one-way (**b**,**c**,**f**) ANOVA with Tukey post-hoc tests. N.D., not determined; N.S., not significant. Graphs indicate mean +/− s.e.m.

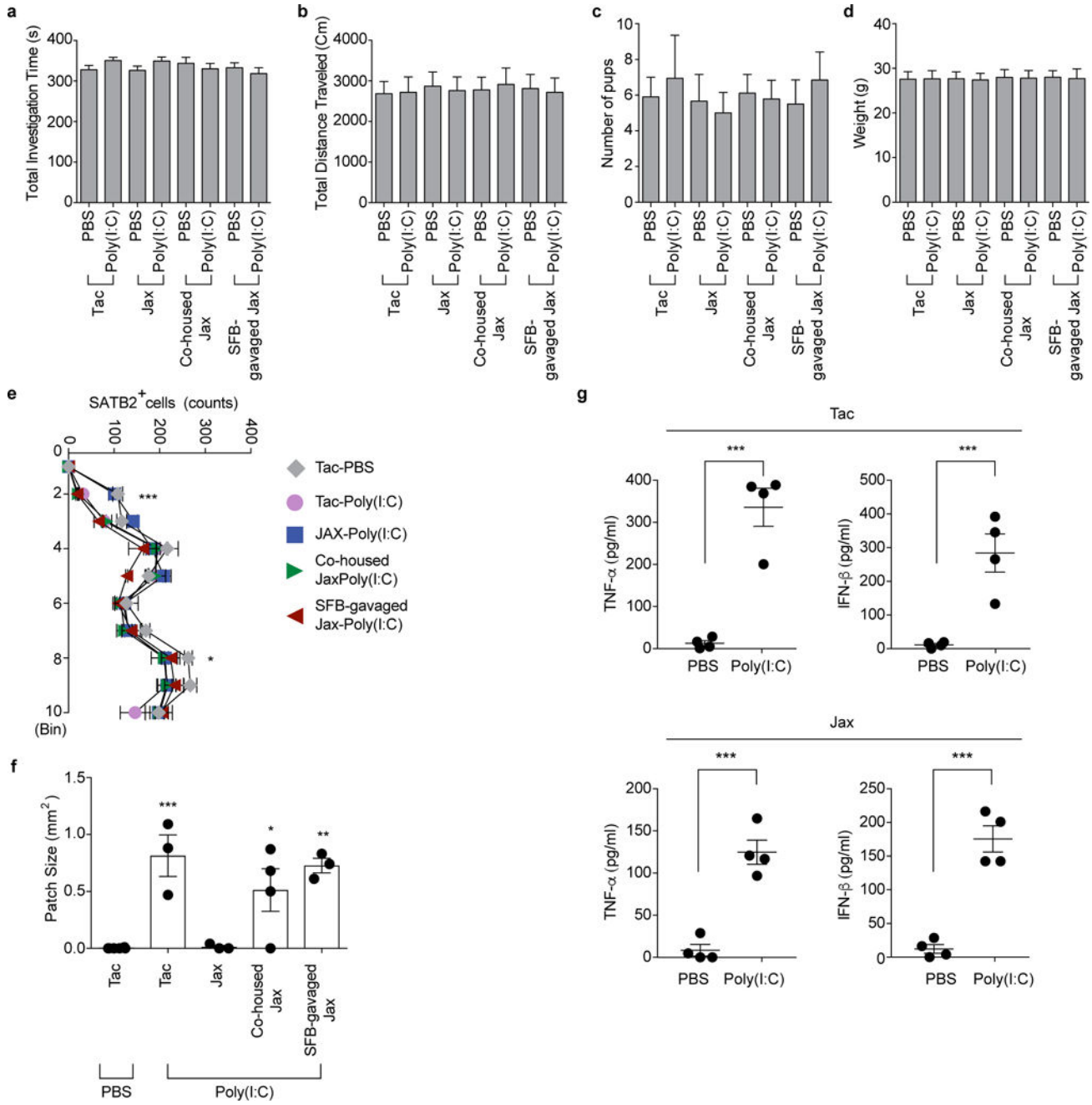

Extended Data Figure 2. MIA in SFB-absent Jax mothers does not induce changes in the total activity of the adult offspring, properties of the litter and maternal cytokine production

a-b, Total investigation time (**a**) and total distance traveled (**b**) during the sociability test. **c**, Litter size upon weaning (*n*=59/125 (Tac;PBS/poly(I:C)); *n*=51/50 (Jax;PBS/poly(I:C)); *n*=55/81 (Co-housed Jax;PBS/poly(I:C)); *n*=55/89 (SFB-gavaged Jax;PBS/poly(I:C)). **d**, Weight of male offspring from the groups described in (**c**) (*n*=32/50 (Tac;PBS/poly(I:C)); *n*=29/27 (Jax;PBS/poly(I:C)); *n*=29/29 (Co-housed Jax;PBS/poly(I:C)); *n*=33/30 (SFB-gavaged Jax;PBS/poly(I:C)). Data in **a**, **b**, and **d** are from 7-8 independent experiments. **e-f**, Quantification of SATB2$^+$ cells (**e**) in the cortex divided into ten equal bins representing

different depth and of patch size (**f**) in the S1 (n=4 (Tac;PBS); n=3/3/4/3 (Tac/Jax/Co-housed Jax/SFB-gavaged Jax;poly(I:C)). **g**, Maternal plasma concentrations of TNF-α and IFN-β at 3 hrs after PBS/poly(I:C) injection into Tac/Jax dams at E12.5; n=4/group. *p<0.05, **p<0.01, ***p<0.001 as calculated by two-way (**e**) and one-way ANOVA (**a-d,g,f**) with Tukey post-hoc tests and Student's t-test (**g**). N.D., not determined. Graphs indicate mean +/− s.e.m.

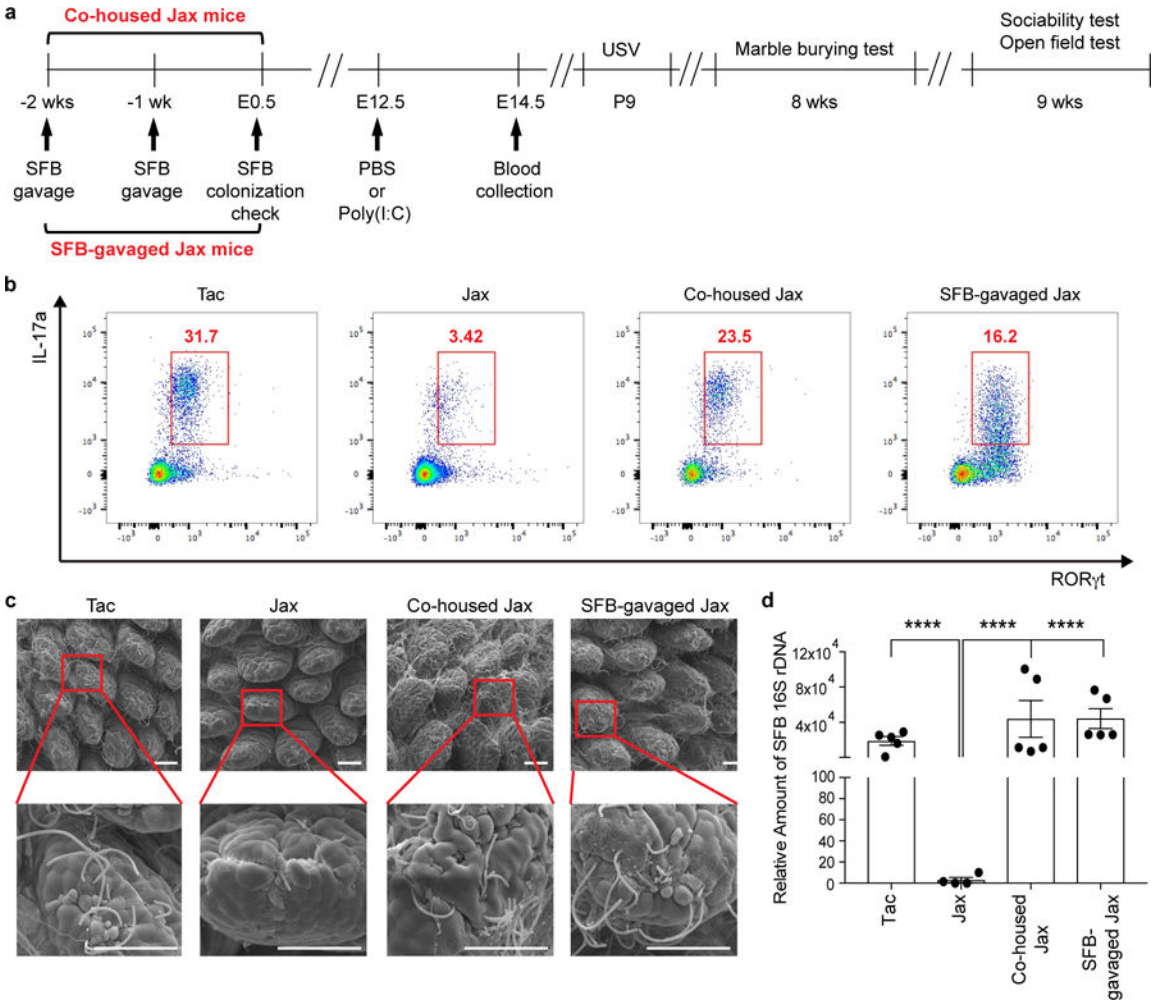

Extended Data Figure 3. SFB colonization leads to increased levels of gut Th17 cells in Jax pregnant mice

a, Schematic of the experimental design. **b.** Flow cytometry of $CD4^+$ T cells (gated on $TCR\text{-}\beta^+CD4^+$) stained intracellularly for IL-17a and RORγt. Mononuclear cells were collected at E14.5 from the ilea of poly(I:C)-treated Tac/Jax/co-housed Jax/SFB-gavaged Jax mothers. **c**, Representative SEM images of epithelial surfaces in the ilea of Tac/Jax/co-housed Jax/SFB-gavaged Jax mothers. Scale bars, 30 μm. Data representative of 3 (**b**) and 2 (**c**) independent experiments. **d**, qPCR analysis for SFB levels in the fecal samples of the groups described in (**a**) (n=4-5/group). ****p<0.0001 as calculated by one-way (**d**) ANOVA with Tukey post-hoc test. Graphs indicate mean +/− s.e.m.

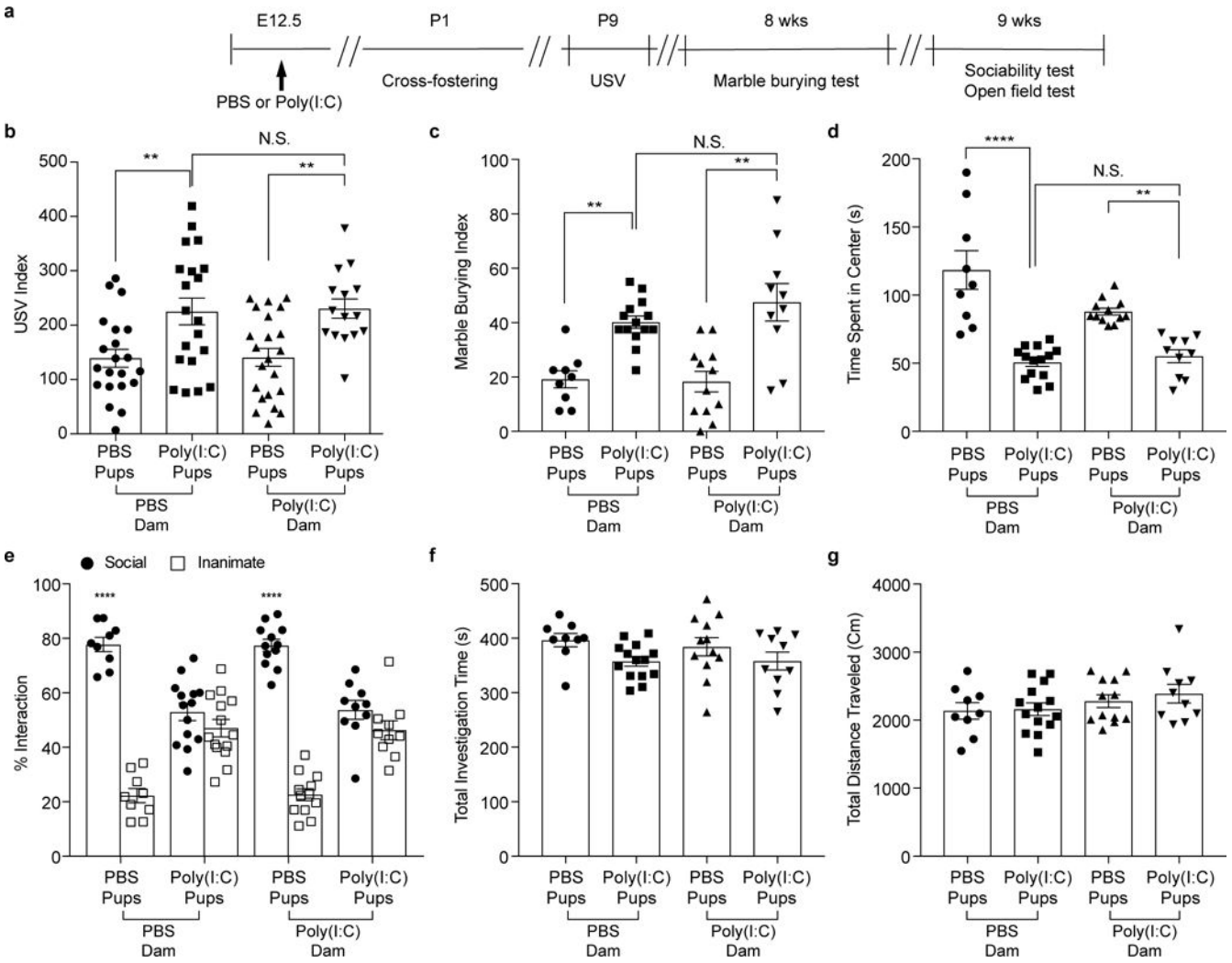

Extended Data Figure 4. Poly(I:C)-induced inflammation during pregnancy, not after giving birth, is critical in inducing MIA-associated behavioral abnormalities in offspring

a, Schematic of the experimental design for cross-fostering experiments. **b**, USV index (n=21/20 (PBS dams;PBS/poly(I:C) pups); n=22/15 (poly(I:C) dams;PBS/poly(I:C) pups); 2-4 independent experiments). **c-g** Marble-burying index (**c**), time spent in the center of an open field (**d**), and % interaction (**e**), total investigation time (**f**), and total distance traveled (**g**) during the sociability test (n=9/14 (PBS dams;PBS/poly(I:C) pups); n=12/10 (poly(I:C) dams;PBS/poly(I:C) pups); 2 independent experiments). **p<0.01, ****p <0.0001 as calculated by one-way (**b-d,f-g**) and two-way (**e**) ANOVA with Tukey post-hoc tests. N.S., not significant. Graphs indicate mean +/− s.e.m.

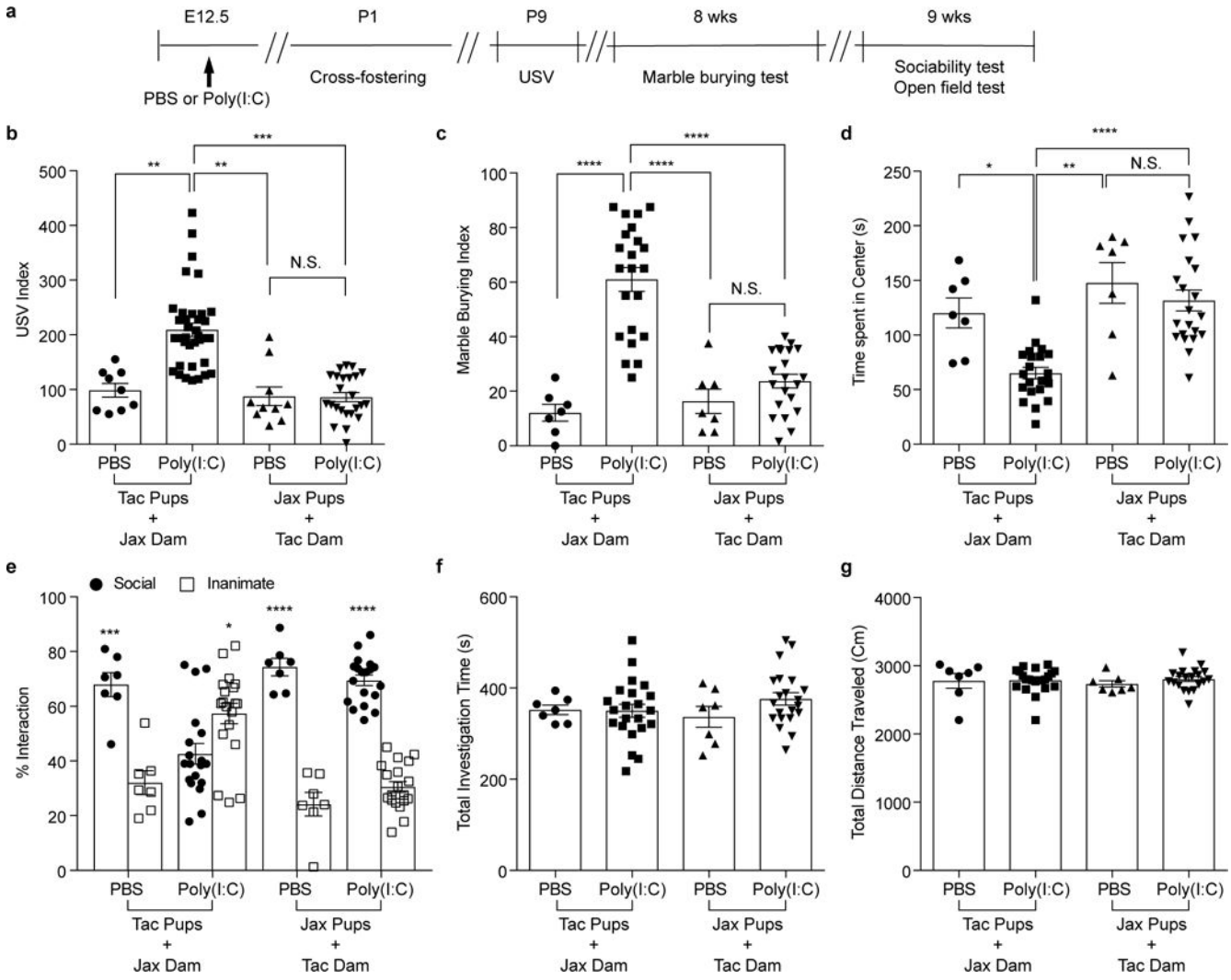

Extended Data Figure 5. Composition of maternal gut microbiota during pregnancy, not after giving birth, is critical in inducing MIA-associated behavioral abnormalities in offspring

a, Schematic of the experimental design for cross-fostering experiments. **b**, USV index (n=9/36 (Tac pups with Jax dams;PBS/poly(I:C)); n=10/24 (Jax pups with Tac dams;PBS/poly(I:C)); 2-4 independent experiments). **c-g**, Marble-burying index (**c**), time spent in the center of an open field (**d**), and % interaction (**e**), total investigation time (**f**), and total distance traveled (**g**) during the sociability test (n=7/22 (Tac pups with Jax dams;PBS/poly(I:C)); n=7/21 (Jax pups with Tac dams;PBS/poly(I:C)); 2 independent experiments). *p<0.05, **p<0.01, ***p<0.001, ****p <0.0001 as calculated by one-way (**b-d,f-g**) and two-way (**e**) ANOVA with Tukey post-hoc tests. Graphs indicate mean +/− s.e.m.

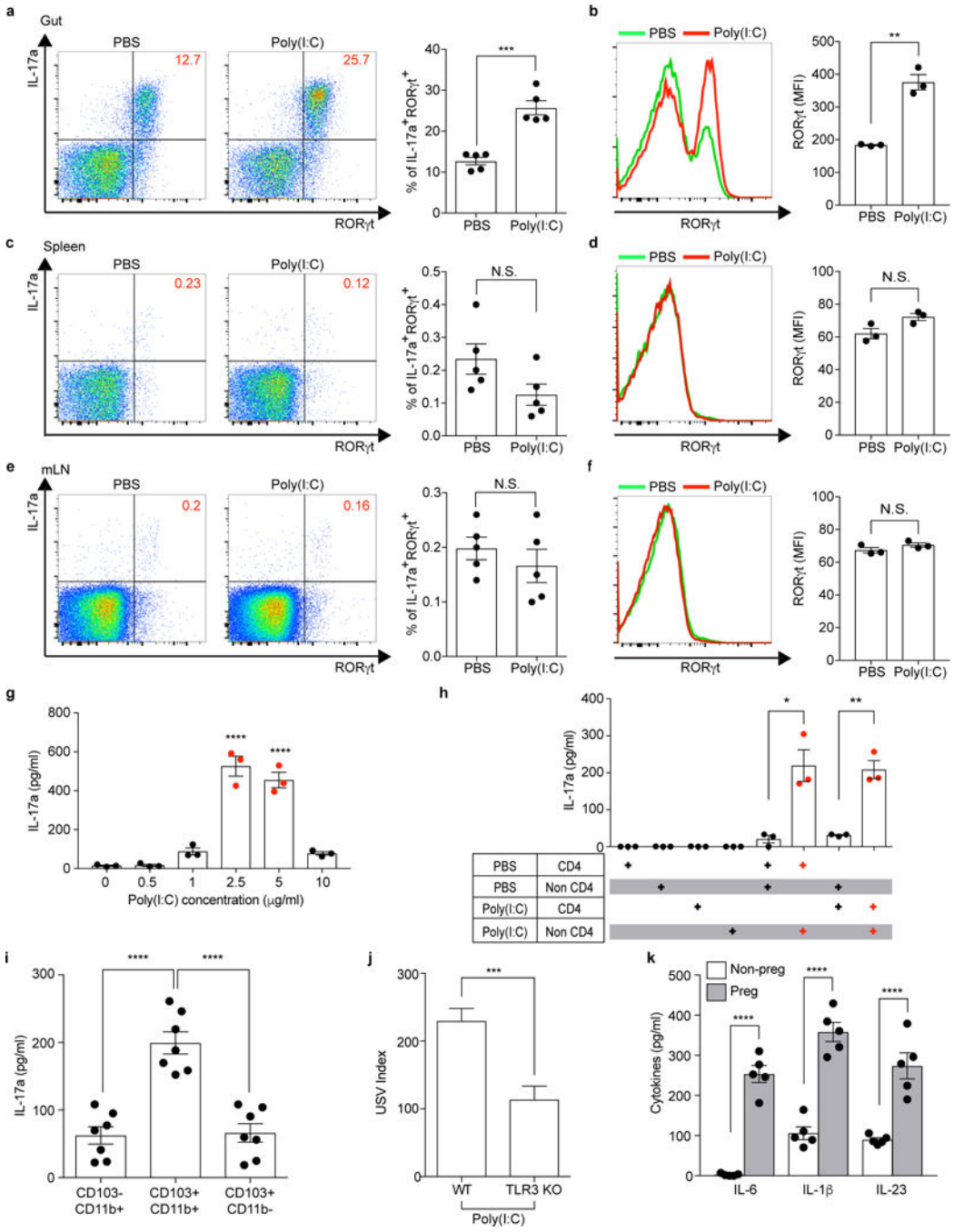

Extended Data Figure 6. CD11c$^+$ cells stimulate gut-Th17 cells to produce high levels of IL-17a *ex vivo*

a-f, Flow cytometry of CD4$^+$ T cells (gated on TCR-β$^+$CD4$^+$) stained intracellularly for IL-17a and RORγt. Mononuclear cells were collected at E14.5 from the gut ilea, spleens, and mesenteric lymph nodes (mLN) of PBS-/poly(I:C)-treated mice (n=5/group (**a, c, e**); n=3/group (**b, d, f**)). MFI denotes mean fluorescence intensity. **g-i**,, Supernatant concentrations of IL-17a from mononuclear cells of the ilea in poly(I:C)-treated Tac dams (**g**) (n=3/group), from co-cultures of CD4$^+$ and non-CD4$^+$ cells of the ilea in PBS-/

poly(I:C)-treated Tac dams (**h**) (n=3/group), or from co-cultures of $CD4^+$ and $CD103^-CD11b^+$/$CD103^+CD11b^+$/$CD103^+CD11b^-$ (gated on $MHCII^+CD11c^+$) cells of the ilea in poly(I:C)-treated dams (**i**) (n=7/group). All cultures were isolated at E14.5 and stimulated *ex vivo* with poly(I:C) for 18hrs (**g-h**) or for 48hrs (**i**). Data are pooled from 2 (**g-h**) or 3 (**i**) independent experiments. **j**. USV index (n=16/17 (poly(I:C);WT/TLR3 KO); 2 independent experiments). **k**, Supernatant concentrations of IL-6, IL-1β, and IL-23 from cultures of $CD11c^+$ isolated at E14.5 from the ilea of poly(I:C)-treated non-pregnant/pregnant mice (n=5/group; 3 independent experiments). *p<0.05, **p<0.01, ***p<0.001 and ****p<0.0001 as calculated by Student's t-test (**a-f,j,k**) and one-way ANOVA (**g-i**) with Tukey post-hoc tests. N.S., not significant. Graphs indicate mean +/− s.e.m.

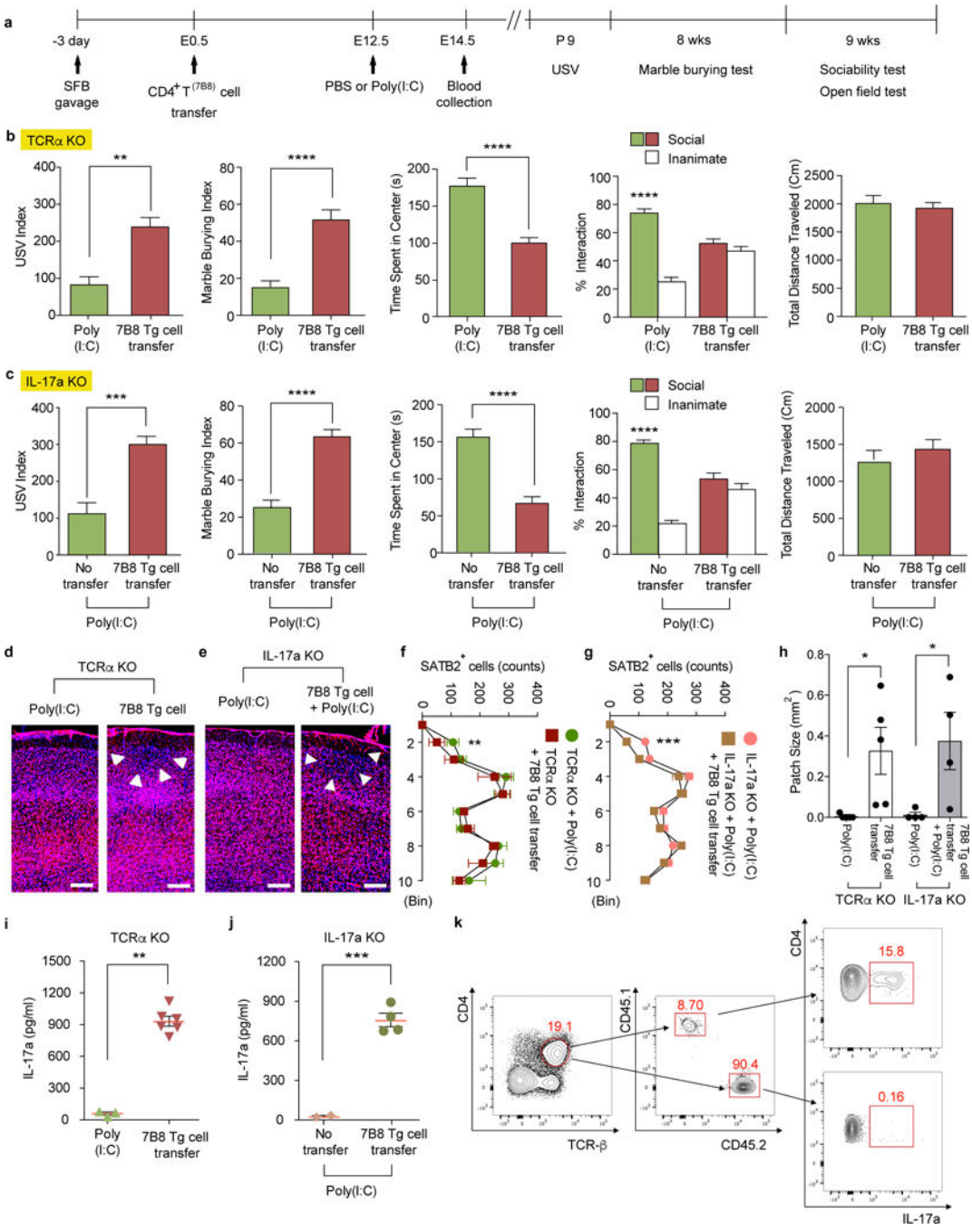

Extended Data Figure 7. SFB-specific 7B8 Tg CD4$^+$ T cells produce IL-17a upon transfer to MIA-exposed pregnant mothers

a, Schematic of the experimental design. **b-c**, Both TCRα KO and IL-17a KO females, with or without adoptive transfers of 7B8 Tg-derived CD4$^+$ T cells, were crossed with B6 WT males to produce heterozygous WT offspring. USV index (n=16/30 (TCRα KO; poly(I:C)/7B8 Tg T cell transfer); n=23/23 (IL-17a KO;poly(I:C)/7B8 Tg T cell transfer), marble burying index, time spent in the center of an open field, and % interaction and total distance traveled during the sociability test of TCRα KO (**b**) or IL-17a KO (**c**) offspring

(*n*=12/15 (TCRα KO; poly(I:C)/7B8 Tg T cell transfer); *n*=12/14 (IL-17a KO;poly(I:C)/7B8 Tg T cell transfer). Data pooled from 2-3 independent experiments. **d-e**, Representative SATB2 staining in the cortex of the animals prepared as in (**a**). Arrows indicate cortical patches. Scale bar, 100 μm. **f-g**, Quantification of SATB2$^+$ cells (*n*=7/6 (TCRα KO;poly(I:C)/7B8 Tg T cell transfer); *n*=6/7 (IL-17a KO;poly(I:C)/7B8 Tg T cell transfer). **h**, Cortical patch size (*n*=5/5 (TCRα KO;poly(I:C)/7B8 Tg T cell transfer); *n*=4/4 (IL-17a KO;poly(I:C)/7B8 Tg T cell transfer). **i-j**, IL-17a concentrations in maternal plasma collected at E14.5. **k**, Flow cytometry of ileal CD4$^+$ T cells (gated on CD4$^+$TCR-β$^+$) stained intracellularly for IL-17a. Mononuclear cells were collected from small intestines of poly(I:C)-treated IL-17a KO mothers transferred with 7B8 Tg CD4$^+$ T cells. CD45.1$^+$ cells refer to donor cells and CD45.2$^+$ to recipient cells. *p<0.05, **p<0.01, ***p<0.001, ****p<0.0001 as calculated by Student's t-test (**b-c,h-j**) and one-way (**f-g**) ANOVA with Sidak post-hoc tests. Graphs indicate mean +/− s.e.m.

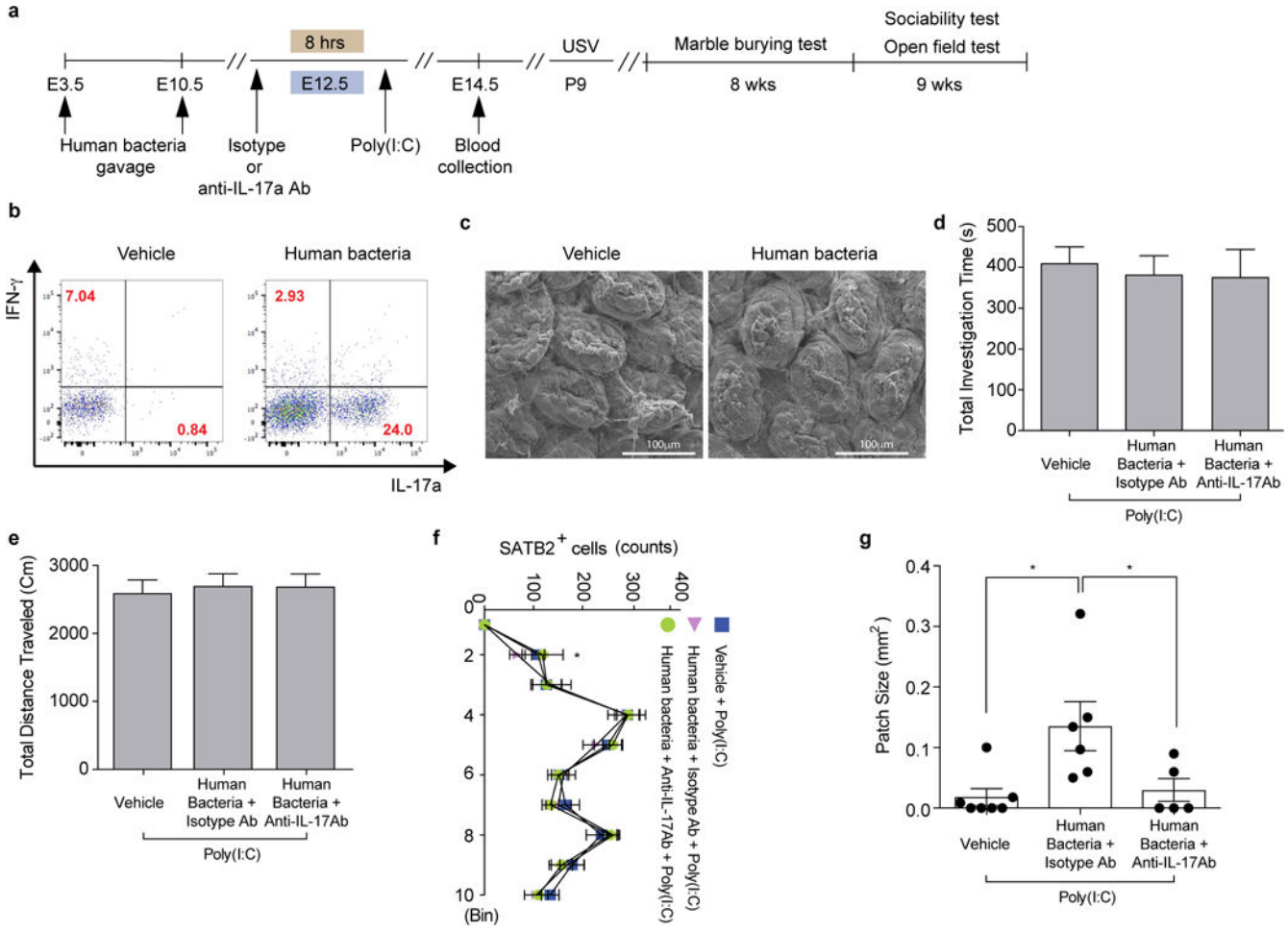

Extended Data Figure 8. A mix of twenty human commensals induces colonic Th17 cell differentiation in SFB-absent Jax mice

a, Schematic of the experimental design. **b**, Flow cytometry of CD4$^+$ T cells (gated on CD4$^+$TCR-β$^+$) stained intracellularly for IL-17a and RORγt. Mononuclear cells were collected from colons of poly(I:C)-treated Jax mothers with/without human bacteria-gavage.

c, Representative SEM images of epithelial surfaces in the ilea from 2 independent experiments. **d-e**, Total interaction time (**d**), and total distance traveled (**e**) during the sociability test of adult offspring described in (**a**) (n=23/22/13 for vehicle-gavaged only/human bacteria-gavaged+isotype control antibody/human bacteria-gavaged+anti-IL-17a antibody; 4 independent experiments). **f-g**, Quantification of SATB2$^+$ cells (n=5/group) and cortical patch size (n=7/6/5 (poly(I:C);vehicle-treated Jax/human bacteria-gavaged Jax with isotype control antibody/human bacteria-gavaged Jax with anti-IL-17a antibody). *p<0.05 as calculated by one-way (**d, e, g**) and two-way (**f**) ANOVA with Tukey post-hoc test. Graphs indicate mean +/− s.e.m.

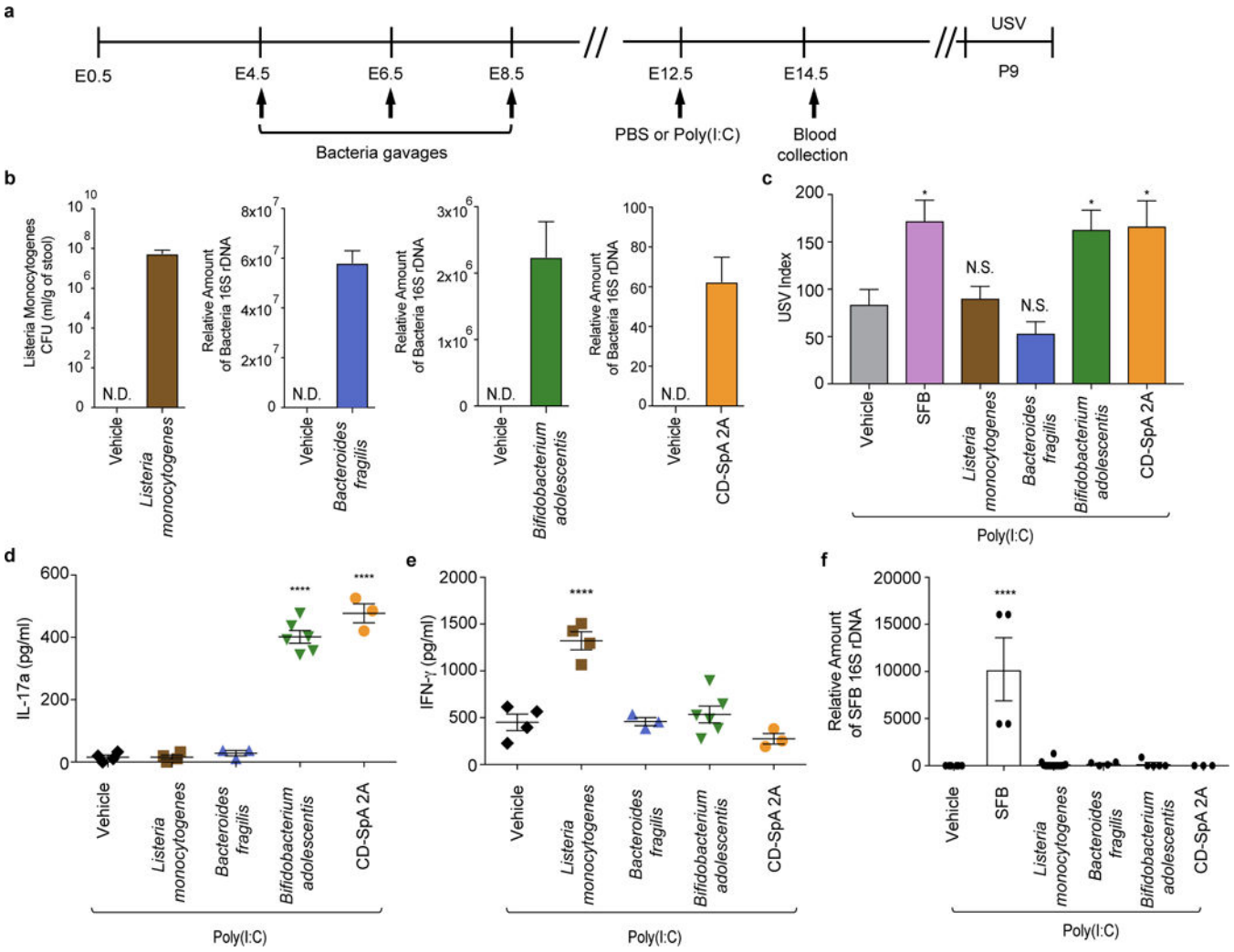

Extended Data Figure 9. The IL-17a pathway promotes abnormal behavioral phenotypes in MIA offspring born to mice colonized with human commensal bacteria

a, Schematic representation of the experimental design. **b**, Quantification of bacterial colonization levels through colony forming unit (CFU) counts or qPCR analyses. **c**, USV index (n=13/12/28/16/17/14 (poly(I:C);vehicle/SFB/*Listeria monocytogenes*/*Bacteroides fragilis*/*Bifidobacterium adolescentis*/CD-SpA 2A). **d-e**, Maternal plasma concentrations of IL-17a/IFN-γ at E14.5 (n=4/4/3/6/3 (poly(I:C);vehicle/*Listeria monocytogenes*/*Bacteroides*

fragilis/Bifidobacterium adolescentis/CD-SpA 2A). **f**, qPCR analysis measuring relative SFB levels in Jax mice gavaged with various bacteria; from two independent experiments. *p<0.05, ****p<0.0001 as calculated by one-way (**c-f**) ANOVA with Tukey post-hoc tests and Student's t-test (**b**). N.D., not determined. N.S., not significant. Graphs indicate mean +/− s.e.m.

Supplementary Material

Refer to Web version on PubMed Central for supplementary material.

Acknowledgments

We thank S. Hang, D. Paik and N. Silverstein for valuable discussions and Y. Yang, M. Xu, N. Geva-Zatorsky, D. Kasper, C. Benoist and D. Mathis for reagents. We thank M. Trombly, N. Silverstein and A. Park for critical reading of the manuscript. We also thank E. Bridge, E. Jaskolski and other staff members at the Department of Animal Medicine at University of Massachusetts Medical School. This work was supported by the Simons Foundation Autism Research Initiative (D.R.L. and J.R.H.), the Simons Foundation to the Simons Center for the Social Brain at MIT (Y.S.Y., J.R.H and G.B.C.), Hock E. Tan and K. Lisa Yang Center for Autism Research (G.B.C.), the Howard Hughes Medical Institute (D.R.L.), Robert Buxton (G.B.C.), the National Research Foundation of Korea grants MEST-35B-2011-1-E00012 (S.K.) and NRF-2014R1A1A1006089 (H.K.), the Searle Scholars Program (J.R.H.), the Pew Scholar for Biomedical Sciences (J.R.H.), the Kenneth Rainin Foundation (J.R.H.), and the National Institutes of Health grants R01DK106351 and R01DK110559 (J.R.H.).

References

1. Machado CJ, Whitaker AM, Smith SE, Patterson PH, Bauman MD. Maternal immune activation in nonhuman primates alters social attention in juvenile offspring. Biological psychiatry. 2015; 77:823–832. DOI: 10.1016/j.biopsych.2014.07.035 [PubMed: 25442006]
2. Bauman MD, et al. Activation of the maternal immune system during pregnancy alters behavioral development of rhesus monkey offspring. Biological psychiatry. 2014; 75:332–341. DOI: 10.1016/j.biopsych.2013.06.025 [PubMed: 24011823]
3. Smith SEP, Li J, Garbett K, Mirnics K, Patterson PH. The Journal of neuroscience : the official journal of the Society for Neuroscience. 2007; 27:10695–10702. [PubMed: 17913903]
4. Malkova NV, Yu CZ, Hsiao EY, Moore MJ, Patterson PH. Maternal immune activation yields offspring displaying mouse versions of the three core symptoms of autism. Brain Behav Immun. 2012; 26:607–616. DOI: 10.1016/j.bbi.2012.01.011 [PubMed: 22310922]
5. Lee BK, et al. Maternal hospitalization with infection during pregnancy and risk of autism spectrum disorders. Brain, behavior, and immunity. 2015; 44:100–105. DOI: 10.1016/j.bbi.2014.09.001
6. Brown AS, et al. Elevated maternal C-reactive protein and autism in a national birth cohort. Molecular psychiatry. 2014; 19:259–264. DOI: 10.1038/mp.2012.197 [PubMed: 23337946]
7. Atladottir HO, et al. Maternal infection requiring hospitalization during pregnancy and autism spectrum disorders. J Autism Dev Disord. 2010; 40:1423–1430. DOI: 10.1007/s10803-010-1006-y [PubMed: 20414802]
8. Choi GB, et al. The maternal interleukin-17a pathway in mice promotes autism-like phenotypes in offspring. Science. 2016; 351:933–939. DOI: 10.1126/science.aad0314 [PubMed: 26822608]
9. Schwartzer JJ, et al. Maternal immune activation and strain specific interactions in the development of autism-like behaviors in mice. Translational psychiatry. 2013; 3:e240. [PubMed: 23481627]
10. Yee N, Schwarting RK, Fuchs E, Wohr M. Increased affective ultrasonic communication during fear learning in adult male rats exposed to maternal immune activation. Journal of psychiatric research. 2012; 46:1199–1205. DOI: 10.1016/j.jpsychires.2012.05.010 [PubMed: 22687817]
11. Casanova MF, et al. Focal cortical dysplasias in autism spectrum disorders. Acta neuropathologica communications. 2013; 1:67. [PubMed: 24252498]

12. Stoner R, et al. Patches of disorganization in the neocortex of children with autism. The New England journal of medicine. 2014; 370:1209–1219. DOI: 10.1056/NEJMoa1307491 [PubMed: 24670167]
13. Ivanov II, et al. Specific microbiota direct the differentiation of IL-17-producing T-helper cells in the mucosa of the small intestine. Cell host & microbe. 2008; 4:337–349. DOI: 10.1016/j.chom.2008.09.009 [PubMed: 18854238]
14. Ivanov II, et al. Induction of intestinal Th17 cells by segmented filamentous bacteria. Cell. 2009; 139:485–498. DOI: 10.1016/j.cell.2009.09.033 [PubMed: 19836068]
15. Lewis KL, et al. Notch2 receptor signaling controls functional differentiation of dendritic cells in the spleen and intestine. Immunity. 2011; 35:780–791. DOI: 10.1016/j.immuni.2011.08.013 [PubMed: 22018469]
16. Persson EK, et al. IRF4 transcription-factor-dependent CD103(+)CD11b(+) dendritic cells drive mucosal T helper 17 cell differentiation. Immunity. 2013; 38:958–969. DOI: 10.1016/j.immuni.2013.03.009 [PubMed: 23664832]
17. Alexopoulou L, Holt AC, Medzhitov R, Flavell RA. Recognition of double-stranded RNA and activation of NF-kappaB by Toll-like receptor 3. Nature. 2001; 413:732–738. DOI: 10.1038/35099560 [PubMed: 11607032]
18. Awasthi A, Kuchroo VK. Th17 cells: from precursors to players in inflammation and infection. Int Immunol. 2009; 21:489–498. DOI: 10.1093/intimm/dxp021 [PubMed: 19261692]
19. Yang Y, et al. Focused specificity of intestinal TH17 cells towards commensal bacterial antigens. Nature. 2014; 510:152–156. DOI: 10.1038/nature13279 [PubMed: 24739972]
20. Nakae S, et al. Antigen-specific T cell sensitization is impaired in IL-17-deficient mice, causing suppression of allergic cellular and humoral responses. Immunity. 2002; 17:375–387. [PubMed: 12354389]
21. Atarashi K, et al. Th17 Cell Induction by Adhesion of Microbes to Intestinal Epithelial Cells. Cell. 2015; 163:367–380. DOI: 10.1016/j.cell.2015.08.058 [PubMed: 26411289]
22. Tan TG, et al. Identifying species of symbiont bacteria from the human gut that, alone, can induce intestinal Th17 cells in mice. Proc Natl Acad Sci U S A. 2016; 113:E8141–E8150. DOI: 10.1073/pnas.1617460113 [PubMed: 27911839]
23. Viladomiu M, et al. IgA-coated E. coli enriched in Crohn's disease spondyloarthritis promote TH17-dependent inflammation. Sci Transl Med. 2017; 9
24. Lee YK, Menezes JS, Umesaki Y, Mazmanian SK. Proinflammatory T-cell responses to gut microbiota promote experimental autoimmune encephalomyelitis. Proceedings of the National Academy of Sciences of the United States of America. 2011; 108(Suppl 1):4615–4622. DOI: 10.1073/pnas.1000082107 [PubMed: 20660719]
25. Wu HJ, et al. Gut-residing segmented filamentous bacteria drive autoimmune arthritis via T helper 17 cells. Immunity. 2010; 32:815–827. DOI: 10.1016/j.immuni.2010.06.001 [PubMed: 20620945]
26. Sivan A, et al. Commensal Bifidobacterium promotes antitumor immunity and facilitates anti-PD-L1 efficacy. Science. 2015; 350:1084–1089. DOI: 10.1126/science.aac4255 [PubMed: 26541606]
27. Erny D, et al. Host microbiota constantly control maturation and function of microglia in the CNS. Nature neuroscience. 2015; 18:965–977. DOI: 10.1038/nn.4030 [PubMed: 26030851]
28. Diaz Heijtz R, et al. Normal gut microbiota modulates brain development and behavior. Proceedings of the National Academy of Sciences of the United States of America. 2011; 108:3047–3052. DOI: 10.1073/pnas.1010529108 [PubMed: 21282636]
29. Cryan JF, Dinan TG. Mind-altering microorganisms: the impact of the gut microbiota on brain and behaviour. Nature reviews Neuroscience. 2012; 13:701–712. DOI: 10.1038/nrn3346 [PubMed: 22968153]

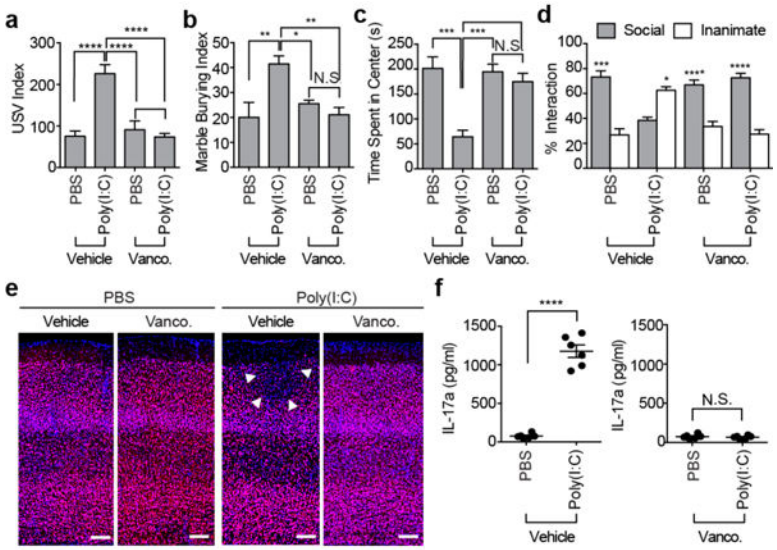

Figure 1. Maternal bacteria promote abnormal behaviors associated with neurodevelopmental disorders in MIA offspring

a, Ultrasonic vocalization (USV) index (n=28/34 (vehicle;PBS/poly(I:C)); n=26/30 (vancomycin;PBS/poly(I:C)); 5-6 independent experiments). **b-d**, Marble-burying index (**b**) time spent in the center of an open field (**c**), % interaction (**d**) in the sociability test of adult offspring described in (**a**) (n=13/15 (vehicle;PBS/poly(I:C)); n=12/16 (vancomycin;PBS/poly(I:C)); 3-4 independent experiments). **e**, Representative images of adult offspring brains from PBS-/poly(I:C)-injected mothers treated with vehicle/vancomycin. Arrows indicate cortical patch. Scale bar,100 μm (n=3/4 (PBS;vehicle/vancomycin); n=5/4 (poly(I:C);vehicle/vancomycin); 2 independent experiments). **f**, Maternal plasma concentrations of IL-17a 48 hrs after PBS/poly(I:C) administration into dams at E12.5 (n=6/group; 3 independent experiments). *p<0.05, **p<0.01, ***p<0.001, ****p<0.0001 as calculated by one-way (**a-c**) and two-way (**d**) ANOVA with Tukey post-hoc tests and Student's t-test (**f**). N.S., not significant. Graphs indicate mean +/− s.e.m.

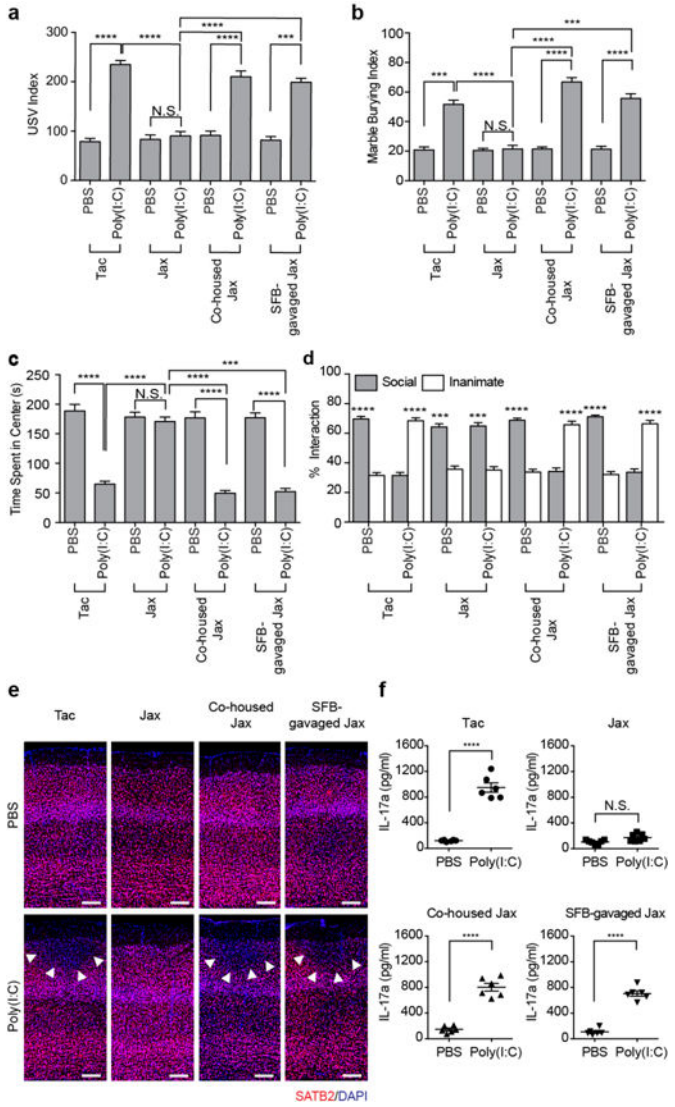

Figure 2. SFB in the pregnant mothers promotes abnormal behaviors in MIA offspring

a, USV index (*n*=59/125 (Tac;PBS/poly(I:C)); *n*=51/50 (Jax;PBS/poly(I:C)); *n*=55/81 (Co-housed Jax;PBS/poly(I:C)); *n*=55/89 (SFB-gavaged Jax;PBS/poly(I:C)); 9-11 independent experiments). **b-d**, Marble burying index (**b**), time spent in the center of an open field (**c**), and % interaction (**d**) in the sociability assay of adult offspring described in (**a**) (*n*=32/50 (Tac;PBS/poly(I:C)); *n*=29/27 (Jax;PBS/poly(I:C)); *n*=29/29 (Co-housed Jax;PBS/poly(I:C)); *n*=33/30 (SFB-gavaged Jax;PBS/poly(I:C)); 7-8 independent experiments). **e**, Representative images of adult offspring brains from PBS-/poly(I:C)-injected mothers. Arrows indicate cortical patches. Scale bar, 100 μm (*n*=3/3 (PBS;Tac/Jax); *n*=3/3 (PBS;co-housed Jax/SFB-gavaged Jax); *n*=4/3 (poly(I:C);Tac/Jax); *n*=3/3 (poly(I:C);co-housed Jax/SFB-gavaged Jax)). **f**, Maternal plasma concentrations of IL-17a 48 hrs after administration of PBS/poly(I:C) into dams at E12.5 (*n*=6/group; 2 independent experiments). ***p<0.001, ****p<0.0001 as calculated by one-way (**a-c**) and two-way (**d**) ANOVA with Tukey post-hoc tests and Student's t-test (**f**). N.S., not significant. Graphs indicate mean +/− s.e.m.

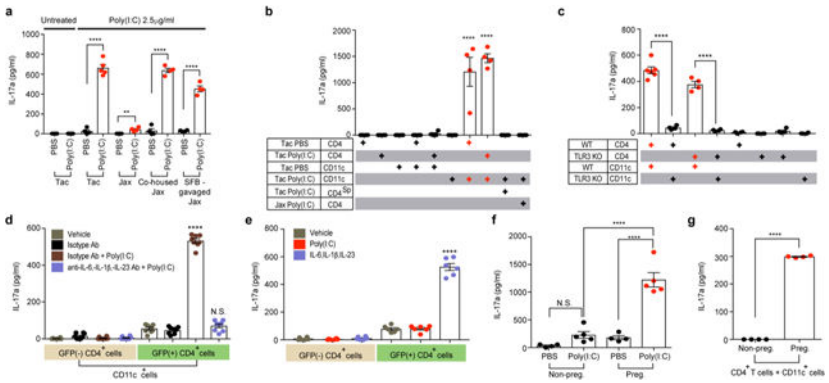

Figure 3. SFB-specific T cells are the major IL-17a producer in pregnant mothers treated with poly(I:C)

a-e,g, Supernatant concentrations of IL-17a from *ex vivo* cultured mononuclear cells of ilea in PBS/poly(I:C)-treated dams (**a**) (n=4-5/group), from co-culture of $CD4^+$ and $CD11c^+$ of ilea in PBS/poly(I:C)-treated Tac/Jax mice (**b**) (n=4/group), from co-cultures of $CD4^+$ and $CD11c^+$ of ilea in poly(I:C)-treated WT/TLR3 KO mice (**c**) (n=4-6/group), from co-cultures of GFP^+CD4^+/GFP^-CD4^+ and $CD11c^+$ from ilea of poly(I:C)-treated *il17a*^{gfp} mice (**d**) (n=8/group), from sorted GFP^+/GFP^-CD4^+ cells (**e**) (n=6/group), or from co-cultures of $CD4^+$ and $CD11c^+$ (**g**) (n=4/group). $CD4^{Sp}$ indicates spleen-derived $CD4^+$ T cells. All cultures were isolated at E14.5 and stimulated with poly(I:C) for 18hrs (**a-c,g**) or for 48hrs (**d-e**). **f**, Maternal plasma concentrations of IL-17a 48 hrs after administration of PBS/poly(I:C) into non-pregnant females or dams at E12.5 (n=4/5 (non-pregnant females;PBS/poly(I:C)); n=4/5 (pregnant females;PBS/poly(I:C))). All data pooled from 2 independent experiments. $^{**}p<0.01$, $^{****}p < 0.0001$ as calculated by one-way (**a-f**) ANOVA with Tukey post-hoc tests and Student's t-test (**g**); N.D., not determined. N.S., not significant. Graphs indicate mean +/− s.e.m.

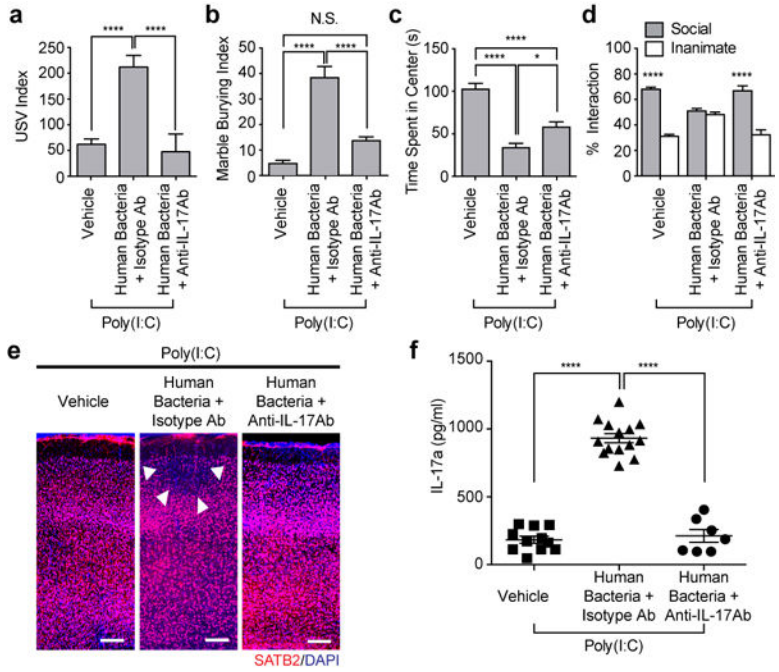

Figure 4. Human commensal bacteria inducing gut Th17 cells promote abnormal behavioral phenotypes in MIA offspring

a, USV index (*n*=38/32/27 for vehicle-gavaged only/human bacteria-gavaged+isotype control antibody/human bacteria-gavaged+anti-IL-17a antibody; 6 independent experiments). **b-d**, Marble burying index (**b**), time spent in the center of an open-field (**c**), and % interaction (**d)** (*n*=23/22/13 for vehicle-gavaged only/human bacteria-gavaged +isotype control antibody/human bacteria-gavaged+anti-IL-17a antibody; 4 independent experiments). **e**, Representative SATB2 staining in the cortex of the offspring derived from vehicle/human bacteria-gavaged Jax dams. Arrows indicate cortical patches. Scale bar, 100μm, **f**. Maternal plasma concentrations of IL-17a at E14.5 (*n*=7-14/group; 2 independent experiments). **p*<0.05, *****p*<0.0001 as calculated by one-way (**a-c, f**) or two-way (**d**) ANOVA with Tukey post-hoc tests. Graphs indicate mean +/− s.e.m.